Eur. Phys. J. Appl. Phys. **30**, 65–73 (2005)
DOI: 10.1051/epjap:2005010

THE EUROPEAN PHYSICAL JOURNAL APPLIED PHYSICS

Influence of the medium rigidity on the growth of multicellular tumor spheroids

M. Griffa[1,2,a], M. Scalerandi[1,2,b], and C. Camagna[1]

[1] INFM - Dept. of Physics, Polytechnic of Torino, C.so Duca degli Abruzzi 24, 10129 Torino, Italy
[2] LIMA Bioinformatics Center, Bioindustry Park of Canavese, Via Ribes 5, 10010 Colleretto Giacosa, TO, Italy

Received: 20 April 2004 / Received in final form: 16 August 2004 / Accepted: 7 October 2004
Published online: 28 January 2005 –

Abstract. The physical interactions of a growing tumor mass with the host tissue (boundary conditions) play an important role in the dynamics of the tumor and their comprehension is essential for designing new therapeutic tools and methods against cancer. Starting from experiments and biological information, we focus here on the analysis of the effects of the coupling between the host's mechanical properties and some relevant cellular processes involved in the growth of multicellular tumor spheroids. The physical-mathematical model proposed here to describe such a coupling and the respective numerical simulations, after validation through a quantitative comparison with experimental data, will be applied to support biological hypotheses previously formulated and to propose new themes of investigation.

PACS. 87.17.Aa Cellular structure and processes: theory and modeling; computer simulation – 87.18.Bb Multicellular phenomena: computer simulation – 87.18.Hf Multicellular phenomena: spatiotemporal pattern formation in cellular populations

1 Introduction

Experimental studies [1–3] have introduced evidences for the influence on tumor growth dynamics of both local biochemical processes and biophysical host tissue's properties. The mechanical opposition to deformations [3,4] and the limited vascularization [5] contribute both to inhibit the growth during the a-vascular phase and influence the tumor morphology and its invasiveness potentialities. From a kinetic point of view, the combined effects of nutrients and space limitations lead to a net balance between the proliferation and the death rates [6], considered the basis for tissue equilibrium.

To develop therapeutic strategies aiming to promote growth inhibition in tumors, it is therefore crucial an understanding of the coupling between physical mechanisms (related e.g. to fluids flow, mechanical compression, molecules diffusion, etc.) and biochemical processes (such as cell metabolism, cell cycle activation, etc.). Unfortunately, the complexity of in vivo conditions makes it difficult a detailed analysis of such a coupling, while in vitro experiments are usually oversimplified. A reasonable compromise is given by Multicellular Tumor Spheroids (MTSs) [1,2,7,8], i.e. spheroidal-like compact aggregates of neoplastic cells grown in a 3D culture medium, which, albeit still in vitro, mimick better in vivo conditions. Mathematical models [9–14] can then support efficiently the experimental analysis, e.g. for studying the mechanical perturbations caused by a tumor mass on the host tissue [15–19] or angiogenesis [20–22].

In this paper, we consider a specific kind of protocol for MTS culture suggested by the experimental work, reported in [2], in which growth inhibition is modulated by controlling the mechanical rigidity of the medium. Referring to that experiment, neoplastic cells are implanted in a polymeric gel (i.e. a stochastic lattice of polymeric fibers and interstitial pores filled with fluids), obtained through a mixture of feeding suspensions and agarose powder. The medium elastic properties can be modulated using a different fraction of agarose powder during the preparation: higher concentrations of agarose correspond to stiffer media [23]. From the experimental data presented in [2], several hypotheses have been formulated about the effects of solid stress on cellular parameters such as the rates of proliferation and apoptosis (cell death caused by DNA damage, or other alterations, occurring during some phases of the cell cycle).

In particular, the apoptotic death seems to be strongly influenced by the degree of cell compaction in the spheroids, since its inhibition is originated by the activation of well defined chemical pathways, which need specific 'ligand-receptor' associations [6,24]. The structure of the surface membrane receptors, usually consisting in

[a] e-mail: michele.griffa@polito.it
[b] e-mail: marco.scalerandi@infm.polito.it

trans-membranal proteins with complex 3D architectures, can be altered in consequence of deformations, so that their specificity to ligands can be lost, with consequent reduction, modification or loss of activation.

We propose a physical-mathematical model to describe the MTS–culture gel interactions. It uses a different approach with respect to some previous papers addressing the same (or similar) kinds of themes [17,19]. Here, we focus on the coupling between mechanical properties and metabolic features, which were neglected elsewhere [17]. Furthermore, at the cost of introducing a less rigorous mathematical model from a continuum mechanics point of view, we present a formulation in which the model parameters may be directly connected with the biological-physical ones and from which a quantitative comparison with experimental data is possible (see Sect. 3).

2 Modeling

We adopt a Population Dynamics approach, i.e. we consider the spheroid like a whole biosystem, even though composed by different kinds of cells, with boundary conditions determined by the culture medium features and the local concentration of nutrients. We include in the formulation only a few cellular and sub-cellular processes ('microscopic' scale, μm), without considering all their details but only the information filtering to cellular clusters ('mesoscopic scale', $\approx$ tens of μm) and then to a 'macroscopic scale', $\approx$ hundreds of μm. By doing that, we renounce to more reliable descriptions, in particular for what concerns the elastic interactions between the spheroid and the medium components, in favor of a more *manageable* model.

2.1 The growth model

2.1.1 Geometrical considerations and notations

Let us consider a spherical 'growth space' of volume V (and diameter D), initially fully replenished of culture medium with the same elastic and geometric properties in each point. V is fixed during the whole experiment. Time is discretized with step Δt (j is the time index) and a cancerous seed is placed in the center of the culture medium at time zero.

To describe the dynamics, we introduce two populations (labeled with an integer $l = 0, 1$):

- $l = 0$, *viable neoplastic cells*: can be either in a quiescent state (also called G_0 phase) or performing the cell cycle (activated phase). In the latter, cells may duplicate or abandon the cycle (at given control points [1,25]) and enter the apoptotic pathway.
- $l = 1$, *apoptotic cells*, i.e. 'entities' obtained from cells after apoptotic death.

The following notations are then introduced:

- $c^j(l) \equiv$ number of cells of type l at time j
- $v_0(l) \equiv$ undeformed volume of a cell of type l
- $v^j(l) \equiv$ volume of cells of type l at time j
- $V^j(l) = c^j(l)\, v^j(l) \equiv$ volume occupied by the population of type l.

A third population is also considered, without space extension and elastic properties: nutrient macromolecular complexes, which, in experiments, are injected in the culture medium and diffuse within it. Let n^j be the nutrient concentration (number per unit volume) at time j and n_0 the concentration at the boundaries of the growth space. A reservoir put in contact with the culture container keeps n_0 constant.

2.1.2 Physical considerations

From a mechanical point of view, each member of the population l ($\forall\, l = 0, 1$) is subjected to a stress $\sigma^j(l)$, defined according to the stress-strain constitutive relation:

$$\sigma^j(l) = s(l)\, \frac{v_0(l) - v^j(l)}{v^j(l)} \tag{1}$$

where $s(l)$ is the elastic modulus. The same formulation is valid for the medium:

$$\sigma_m^j = s_m\, \frac{V - V_m^j}{V_m^j} \tag{2}$$

where s_m is the mean elastic modulus of the culture medium, which depends on the agar concentration, V_m^j is the volume of the culture medium after deformation due to the co-presence of cells in the same total (constant) volume of the 'growth space', V.

As a basic hypothesis, we consider a uniform distribution of mechanical stresses among the populations and the culture medium. Such assumption is reasonable, since the visco-elastic relaxation processes which lead to equilibrium [26,27] are very fast compared to the typical values of the time step Δt of the simulation (see Sect. 3).

The hypothesis of uniform distribution of stress among populations is expressed as:

$$\begin{cases} \sigma^j(0) = \sigma^j(1) \\ \sigma^j(0) = \sigma_m^j \end{cases} \qquad \forall\, j \in N. \tag{3}$$

Equations (1–3) constitute a set of coupled non-linear algebraic equations, with unknowns $v^j(l)$ and V_m^j, which can be solved numerically. Note that equations (1–3) yield that the stress $\sigma^j(l)$ on the cells of the lth population is due to all other cells (and the medium). In fact, $v^j(l)$ depends upon the number of cells of each population through the relation $V = V_m^j + \sum_l c^j(l)\, v^j(l)$.

2.1.3 Constitutive growth equations

We consider the following cellular events.

– *Activation*: each viable cell enters the cellular cycle activated phase with probability p_a^j. It follows that the number of cells activated at time j is

$$c_a^j(0) = p_a^j\, c^j(0). \tag{4}$$

The remaining cells,

$$c_q^j(0) = c^j(0) - c_a^j(0), \tag{5}$$

stay quiescent in the time interval $[j, j+1]$.

– *Apoptotic death*: in the time interval $[j, j+1]$, each activated cell (but not quiescent cells) dies with probability p_d^j. Therefore, the number of dead cells is

$$c_d^j(0) = p_d^j\, c_a^j(0). \tag{6}$$

– *Reproduction*: the activated cells surviving apoptosis

$$c_s^j(0) = c_a^j(0)\,(1 - p_d^j); \tag{7}$$

complete the cell cycle and duplicate.

Note that necrosis, i.e. cell death due to starvation [28], is neglected here. Although necrosis is always present in large spheroids, as we'll see, the mechanical stress applied by the surrounding culture medium limits the spheroid diameter to a few hundreds μm. In these cases experiments show negligible formation of necrosis with respect to larger spheroids [2].

It follows:

$$\begin{cases} c^{j+1}(0) = c_q^j(0) + 2\, c_s^j(0) \\ \\ c^{j+1}(1) = c^j(1)\,(1 - p_r) + c_d^j(0). \end{cases} \qquad \forall\, j \in N \tag{8}$$

The term $p_r\, c^j(1)$ accounts for phagocytosis, a mechanism triggered by cancerous cells both in vitro and in vivo, through which apoptotic masses are removed with probability p_r [29].

Finally, we introduce a (per cell) nutrient consumption parameter γ_{nut}^j, i.e. the number of nutrient molecules captured by each cell in one time step. It follows that the nutrient concentration (i.e. the number of molecules per unit of volume) evolves as

$$n^{j+1} = n^j - \frac{\gamma_{nut}^j\, c^j(0)}{V} + \mu\,(n_0 - n^j), \tag{9}$$

where the last term describes the injection of nutrient from the reservoir in contact with the culture medium through an interface of permeability parameter μ.

2.2 The model of the cellular processes

2.2.1 Modeling molecular uptake

Two processes introduced in the model are triggered by molecules uptake: cellular reproduction and apoptotic death. In the first case, the molecules of interest are nutrient units; in the latter growth factors (emitted by other cells) function like apoptosis inhibitors. We consider a general model for molecular uptaking [21,30] suggested by several experiments [31,32].

The number of molecules captured by each cell, γ, depends from the local availability of molecules χ:

$$\gamma = \Gamma\, \left(1 - \exp\left[-\frac{\chi}{\Gamma\, c(0)}\right]\right) \tag{10}$$

where Γ is the asymptotic (per cell) absorption parameter and the product $\Gamma\, c(0)$ is a 'competition among cells' term.

For the uptake of nutrient units:

$$\gamma_{nut}^j = \Gamma_{nut}\, \left(1 - \exp\left[-\frac{n_{av}^j\, V_s^j}{\Gamma_{nut}\, c^j(0)}\right]\right) \tag{11}$$

where

$$n_{av}^j = \frac{n^j}{\log[k\, s_m]} \tag{12}$$

is the averaged nutrient density (corresponding approximately to the local amount of nutrient available per unit volume). Experimental data [33] show that n_{av}^j decreases slightly with increasing the medium rigidity (through the log term, in which k is a normalization parameter): the agarose gel gets stiffer due to a complexification of the random grid of polymeric fibers and pores, so the diffusivity of macromolecules diminishes, albeit very slowly.

The absorption of apoptosis inhibition molecules can be described accounting for the influences of mechanical deformations on receptors and competition among cancerous cells for survival factors:

$$\gamma_{surv}^j = \Gamma_{surv}^j\, \left(1 - \exp\left[-\frac{\chi_{loc}^j}{\Gamma_{surv}^j\, c^j(0)}\right]\right) \tag{13}$$

where

$$\Gamma_{surv}^j = \xi\, \frac{v^j(0)}{v_0(0)} \tag{14}$$

codifies the role of deformation of the cellular membrane in triggering the efficiency in uptake and

$$\chi_{loc}^j = \xi_1\, (c^j(0))^2 \tag{15}$$

expresses the local amount of survival units. The proportionality to the square of $c^j(0)$ derives from the fact that survival molecules are emitted from neoplastic cells, with a stimulus to production proportional to the local number of cells.

2.2.2 Modeling the probabilities for processes

The probabilities for reproduction and apoptotic death depend on the number of absorbed molecules that function like triggering signals for the specific event.

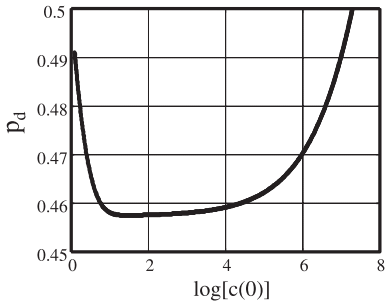

Fig. 1. Behavior of the apoptotic process represented in the $\log(c(0))$ vs. p_d plane, calculated from a simulation with a medium rigidity $\frac{s_m}{s(0)} = 1$. The probability for the apoptotic death decreases with increasing $c(0)$ as long as cells are few enough to have small deformations and the increment of sources for survival factors is dominant. After a configuration of minimum value, p_d increases with increasing $c(0)$, simulating the competition among cells for apoptosis inhibition factors and reduction of uptake efficacy due to receptors buckling.

The probability for cell cycle activation is assumed to be proportional to the nutrient uptake, with a proportionality constant $\frac{1}{\lambda}$:

$$p_a^j \equiv \frac{\gamma_{nut}^j}{\lambda}. \tag{16}$$

For what concerns the apoptosis probability, we introduce a formulation for p_d^j that account for a basic level of apoptosis induction modulated in a strong manner through the social cellular communication [6,34]:

$$p_d^j \equiv \xi_2 \exp[-\gamma_{surv}^j]. \tag{17}$$

In Figure 1, to exemplify, we plot p_d^j as a function of $\log[c(0)]$ as obtained from one simulation (see the related caption).

Finally, the removal of apoptotic units is influenced by the movement of apoptotic residuals which can fluctuate for long time before being recovered and ingested [29]. In vitro such a phagocytosis is only due to the surrounding cancerous cells. Therefore, increasing the structural complexity of the culture medium, the compactness can reduce apoptotic cores mobility and phagocytosis is more frequent. Therefore, we propose

$$p_r \equiv \frac{1}{1 + \exp[-\frac{s_m - h_1}{h_2}]}. \tag{18}$$

The removal probability p_r increases with the medium stiffness but saturate in more rigid media, where apoptotic cores can no longer migrate since the pore radius has become smaller than the typical apoptotic cores dimension.

Table 1. Parameters related to geometrical properties of a typical experiment of MTS growth.

Parameter	Value	Reference and notes
D	10^3 μm	[2,35]
$v_0(0)$	524 μm^3	spheres of diameter 10 μm [36]
$v_0(1)$	524 μm^3	from microscopy techniques, it's shown that dead cores have about the same size as viable cells [29]
$s(0)$	1 KPa	typical order of magnitude [37]
$s(1)$	$2\,s(0)$	[38]

2.3 Parameters analysis

2.3.1 Scaling relations

From equations (3, 12 and 18), we can normalize each elastic modulus as:

$$s_m \to \frac{s_m}{s(0)}$$

$$s(l) \to \frac{s(l)}{s(0)} \qquad \forall\, l = 0, 1$$

$$k \to k \cdot s(0)$$

$$h_i \to \frac{h_i}{s(0)} \qquad i = 1, 2.$$

So, the model results depend only from the ratios of the elastic moduli, more easy to estimate than their absolute values.

Also, from equations (9 and 11) the following coupled scaling can be adopted:

$$\begin{aligned} \Gamma_{nut} &\to \theta \cdot \Gamma_{nut} \\ n_0 &\to \theta \cdot n_0 \\ n^j &\to \theta \cdot n^j \\ \lambda &\to \theta \cdot \lambda. \end{aligned}$$

The results of the simulations are then independent from the scaling parameter θ and one of the model parameter can be fixed arbitrarily. Particularly, the dynamics of the system is governed only by the ratio Γ_{nut}/λ and not by their individual values.

2.3.2 Geometry-related parameters

Some parameters are related with the geometrical properties of the set up to be simulated and can be fixed (at least the typical order of magnitude) for a typical laboratory experiment on MTS growth (see Tab. 1).

Furthermore, the behavior of $\frac{s_m}{s(0)}$ as a function of the agar percent in the medium is exponential [23]:

$$\frac{s_m}{s(0)} = m_1 \exp\left[\frac{\%agar}{m_2}\right]. \tag{19}$$

Reasonable values for s_m are obtained for $m_1 = 3 \times 10^{-4}$ and $m_2 = 8 \times 10^{-2}$.

2.3.3 Biological parameters

Some of the parameters can be fixed considering numerical simulations in specific and simple conditions.

We first consider experiments for the determination of the doubling time, experimentally measured in vitro in the most comfortable conditions for proliferation of the population. For our model, that means considering in equation (8) p_a^j in condition of high abundance of nutrients ($p_a^j = \frac{\Gamma_{nut}}{\lambda}$) and p_d^j set at its minimum allowed value ($p_d^j = \xi_2\, e^{-\xi}$). Using the first of equations (8) and starting from a cancerous seed $c_{ini}(0)$, the cancerous population evolves as

$$c^j(0) = c_{ini}(0)\ \left[1\ +\ \frac{\Gamma_{nut}}{\lambda}\,(1\ -\ 2\,\xi_2\, e^{-\xi})\right]^j. \qquad (20)$$

The number of time steps j_{doubl} necessary for the doubling of the population can be calculated as

$$j_{doubl} = \frac{\log[2]}{\log[1\ +\ \frac{\Gamma_{nut}}{\lambda}\,(1\ -\ 2\,\xi_2\, e^{-\xi})]}. \qquad (21)$$

Likewise, the mean time for the apoptotic mass removal, defined as the number of time steps required for the re-absorption of half the apoptotic population in absence of further apoptosis occurrence (Eq. (8) neglecting the term with c_d^j), can be evaluated as:

$$j_{remov} = -\frac{\log[2]}{\log[1\ -\ p_r]}. \qquad (22)$$

Another biological property is related to turnover. Given a seed of $c_{ini}(0)$ cancer cells, co-occurrence of reproduction and apoptotic death takes place. The total number of cells increases, but the number of them belonging to the initial population decays exponentially with time: after N_r cell cycles the amount of original cells is

$$c(0_{ini}) = c_{ini}(0)\ \exp[N_r\,\xi_2\, e^{-\xi}].$$

p_d acts like a decay time and the number of cell cycle occurring for a typical turnover can be defined as

$$N_{to} = \frac{2}{\xi_2\, e^{-\xi}}. \qquad (23)$$

Beyond those definitions, we impose the condition that with an initial seed of $c_{ini}(0) = 1$ the cancer population can't develop, i.e.

$$\xi_2\ \ \exp\left[-\xi\,\left(1 - \exp\left[-\frac{\xi_1}{\xi}\right]\right)\right] = 0.5. \qquad (24)$$

In Table 2 the measured values of the considered biological quantities are reported together with the corresponding values of the fixed parameters.

Table 2. Parameters estimated from known experimental data.

Experimental Param.	Exp. Value	Model Param.	Ref.
t_{doubl}	23 hours	$\Gamma_{nut} =$	[36]
$= j_{doubl}\Delta t$		$0.15 \cdot \lambda$; (Eq. (21))	
t_{remov}	1–10 hours	$h_2 = 0.38 \cdot h_1$;	[29,39]
$= j_{remov}\Delta t$		(Eq. (22))	
N_{to}	5	$\xi_2 = 0.4 \cdot e^{\xi}$;	
		(Eq. (23))	
		$\xi_1 = 1.5$;	
		(Eq. (24))	

Table 3. Values of the parameters used in the simulations, unless otherwise specified.

Parameter	Value
μ	0.8
$k\, s(0)$	10^5
$h_1/s(0)$	3.5
ξ_3	1

3 Simulations and results

Several simulations have been performed to compare the model results with experimental data taken from [2]. Such comparisons have allowed us to fix the values of the remaining parameters as reported in Table 3.

In addition, we choose a time step $\Delta t \approx 1$ hour, large enough to neglect cellular transitory phenomena and elastic relaxation processes but small enough to appreciate the features of the dynamics of the macroscopic growth.

The initial conditions are defined as

$$\begin{aligned} c^0(0) &= 8 \\ c^0(1) &= 0 \\ n^0 &= n_0 \end{aligned} \qquad (25)$$

where the initial number of cancer cells has been estimated from the spheroids diameters at $t = 0$ in Figure 1 of [2].

3.1 Comparison with experimental data

3.1.1 Dynamics of the virtual MTS

In Figure 2, the number of viable and apoptotic cells are plotted versus time in a semi-log scale for different values of the medium stiffness. Results show that the MTS grows until a steady state configuration (*plateau*). The plateau value depends on the agar concentration in the culture medium. Simulations confirm that the arrest of growth is due to a net equilibrium between proliferation, apoptotic death and apoptotic mass removal.

The qualitative features of the growth (diameter vs. time) confirm an exponential growth with an exponential retardation, characterized by a sigmoidal-like shape (see Fig. 3) [9,12,35]. Simulation results are quantitatively

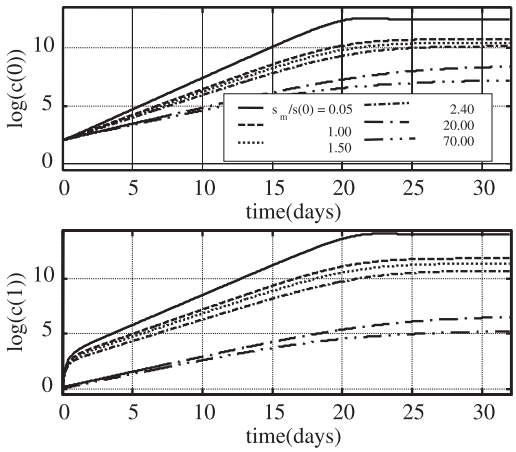

Fig. 2. Time series for the number of viable and apoptotic cells for a spheroid developing in gels with different agarose concentration.

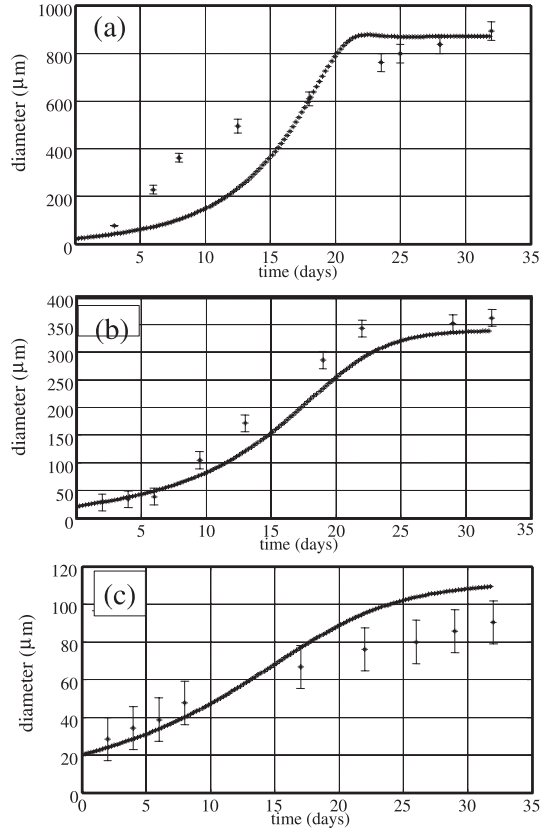

Fig. 3. Time series of the spheroid diameter for different gel cultures. In each plot simulation (stars) and experimental (stars with error bars) data are reported. Experimental data are taken from Figure 1 of reference [2].

comparable with the experimental data, except for Figure 3a, probably due to the absence of a necrotic population in the model that, on the contrary, has been observed in sections of spheroids at *plateau* with the correspondent agar concentration ([2], page 780). In fact, in the absence of agar powder in the gel, the spheroid becomes considerably larger and nutrient deprivation in its core starts

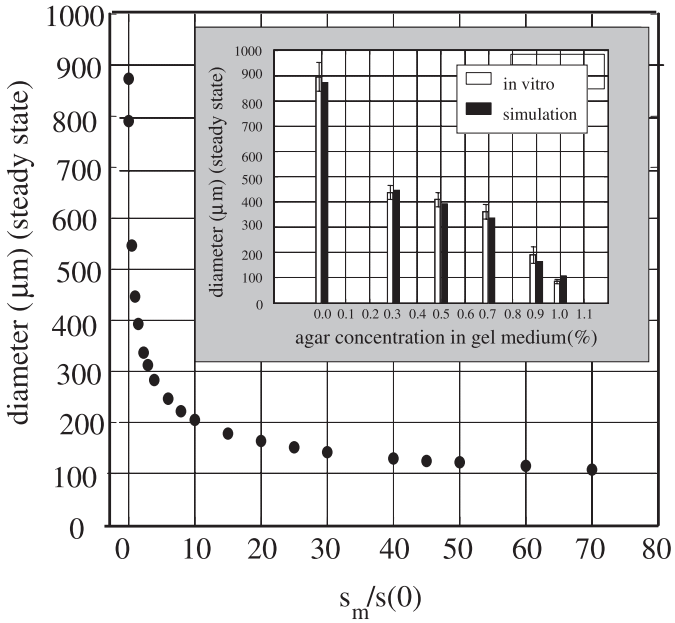

Fig. 4. Diameters of the spheroids at *plateau* vs. medium rigidity. Simulations and experimental data taken from Figure 1 in [2] are compared in the histogram.

being much more considerable and wide. Note that negligible necrosis is found in smaller spheroids.

The time scale of the virtual process is in excellent agreement with the one of real experiments (about 32 days to reach the *plateau* configuration).

3.1.2 Steady state configuration

Figure 4 shows that the virtual MTS diameter (reported vs. $\frac{s_m}{s(0)}$) decreases monotonically when s_m becomes higher, reproducing the mechanical effect of growth inhibition. Numerical results are in excellent agreement with experimental data, as reported in the inset for the available values of agar concentration.

On the contrary, the compactness of the spheroid grows when the gel gets stiffer (see Fig. 5), with results comparable with the experimental data for the corresponding culture gels, as presented in the histograms.

Simulations also reveal that the pressure σ isn't affected by changes in medium stiffness and, for a given stiffness, monotonically increases with increasing the spheroid mass. This result is in agreement with measures reported in Table 1 of reference [2], which show that higher agarose concentrations in the gel do not entail more stress.

As a support to the hypotheses proposed in [1,2,6,24], the model reveals that the opposition to growth from stiffer media has profound implications at the biochemical level. As shown in Figure 6, the probability that a cell enters the activated cycle (normalized to the corresponding probability at 0% agar concentration) decreases monotonically with increasing the medium stiffness, i.e. the onset of cell cycle activation in the viable population

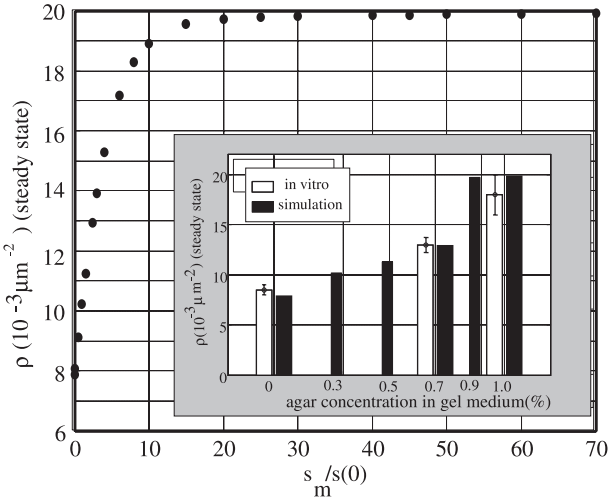

Fig. 5. Compactness (surface density) of the spheroid at *plateau* vs. medium stiffness. The experimental data in the histograms are taken from [2].

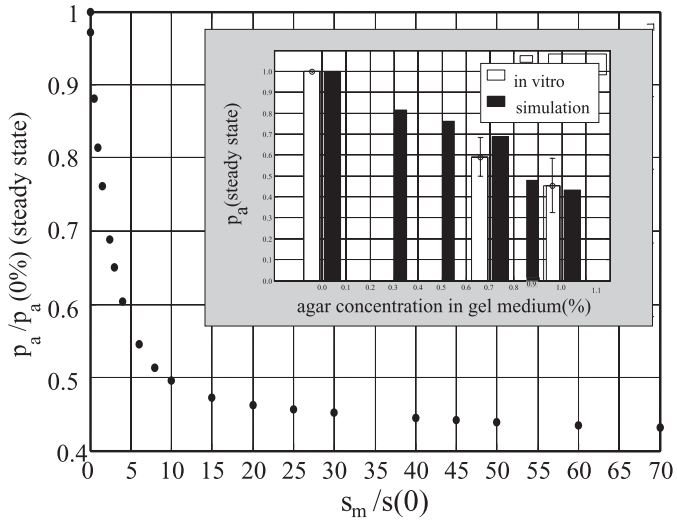

Fig. 6. p_a (normalized to its value in free suspension) at the steady state vs. medium rigidity. Simulation and experimental data are compared in the histogram [experimental data are taken from Fig. 3a of [2]]. Data are normalized to obtain absolute values independent on the typical time decays associated with fluorescence processes used for labeling and enumerating cells.

is inhibited by the compactness of the spheroid, as confirmed by experimental data [1]. Again, the quantitative agreement with available experimental data is excellent (see inset).

3.2 In silico experiments

After validation, the model can be used to perform virtual experiments, starting from the set up of parameters previously presented (from now on called *benchmark* values).

We first investigate the role of the parameter λ, which by definition is associated with the metabolic properties of neoplastic cells, so that different cell lines can be simulated by distinct λ values. Figure 7a shows that the parameter controls the kinetics, but not the steady state condition. In fact, more demanding cells (higher values of λ) take longer to reach the same population level but the final volume of the spheroid is the same. Similar results are obtained varying Γ_{nut}, while the final volume is extremely sensitive to other intrinsic cell parameters [28].

In addition, we analyze the influence of λ on proliferation (Fig. 7b). To this purpose, we introduce the variable:

$$U_{prolif} = \frac{\log[2]}{\log[1 + p_a^{j_{plateau}}]} \Delta t, \tag{26}$$

where $p_a^{j_{plateau}}$ is the activation rate calculated at *plateau*. U_{prolif} can be considered as an 'estimator' parameter for the slow-down of the proliferation of the viable population when the MTS achieves the quiescent configuration. It can be used as a grading parameter of tumor nodules. In Figure 7b U_{prolif} is plotted versus λ for different media. Results show that higher values of λ can be considered less dangerous, because cells are more demanding of nutrient to proliferate: increasing λ the process is slower (Fig. 7a) and the doubling time higher (Fig. 7b). But the prediction of the tumor aggressiveness accounting only cell parameters (λ, or any other) is not reliable [40]. In particular, the host elastic properties influence the tumor malignancy: the tumor aggressiveness is decreased when the tumor grows in a stiffer medium. For example, an in principle less aggressive tumor (e.g. $\lambda = 150$) in a rigid tissue (e.g. $\frac{s_m}{s(0)} = 7.5$) may result less dangerous than a tumor with $\lambda = 212$ in a softer host ($\frac{s_m}{s(0)} = 1$).

By varying n_0 around its *benchmark* value ($n_{0benchmark} \approx 9.88 \times 10^9$ mm^{-3}), we show in Figures 8a and b both the huge effects of nutrient shortage (decreasing n_0) and the scarce importance of further increase of n_0 (*saturation effect*). In Figure 8a (percent variation of the number of viable cancer cells at *plateau* with respect to the *benchmark* vs. $\frac{n_0}{n_{0benchmark}}$), the limiting effect on the upper levels reachable by the MTS due to nutrients deprivation is visible. Note the slight effect of n_0 when $n_0 > n_{0benchmark}$. The saturation effect (large n_0) is more easily seen in Figure 8b (spheroid diameter vs. $\frac{s_m}{s(0)}$ for different $\frac{n_0}{n_{0benchmark}}$): curves almost collapse for $n_0 \geq 0.8 n_{0benchmark}$. Figure 8b shows also that the medium rigidity significantly influences the MTS dimension only when n_0 is large: the nutrient availability parameter behaves like a pre-condition for growth, in the absence of which the spheroid doesn't have a sufficient 'internal energy' for proliferation to really appreciate the medium opposition. Likewise, as also visible in Figure 8a, the effects of nutrient scarcity is relevant mostly for soft hosts. Note also that, for $n_0 < n_{0\ benchmark}$ the MTS grows more slowly (not reported).

The third kind of in silico experiments are concerned with the analysis of the role of apoptotic mass removal: by increasing the parameter h_2, the mechanism of reabsorption becomes less efficient. Mass removal influences not only the kinetics and quality of development, but also

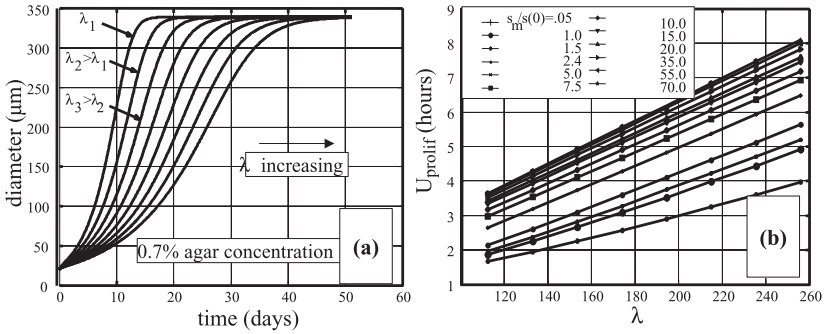

Fig. 7. Dependence on the parameter λ. (a) time series for the diameter of a virtual spheroid growing in a 0.7% agar medium for different values of λ; (b) dependence of the 'proliferation potential' parameter, (Eq. (3.2)), on λ for different values of the medium stiffness. Higher values of U_{prolif} mean less malignancy.

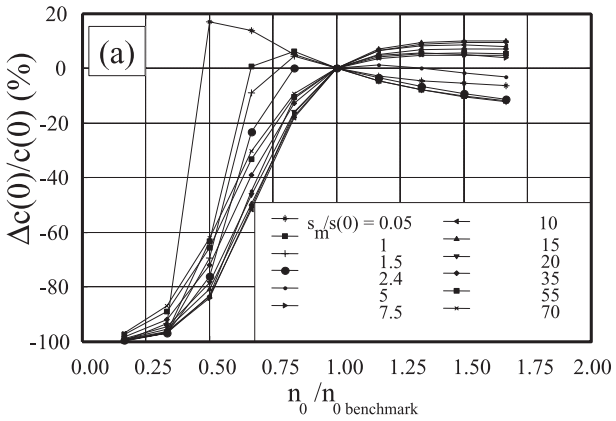

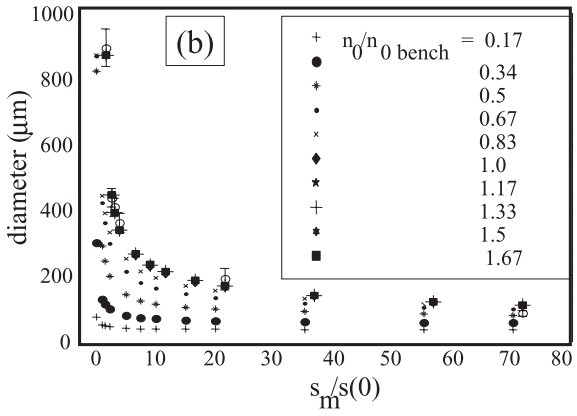

Fig. 8. Influence of the nutrient availability n_0. (a) relative variations of $c(0)$ at *plateau* from the benchmark value for different medium rigidities; (b) spheroid diameter at *plateau* vs. medium rigidity for different values of n_0.

the distribution of deformations among the populations and the compactness of MTS, as shown in Figure 9, where the density ρ at steady state is reported vs. h_2. The density decreases monotonically, i.e. the removal kinetics regulate competition between units of different populations for space occupation and, consequently, control both the reproduction rates and the response to opposition of the medium to elastic deformation.

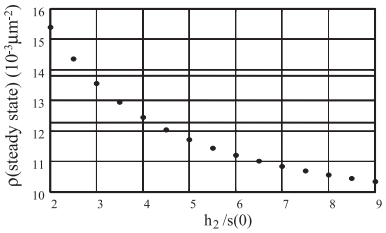

Fig. 9. Influence of the mass removal mechanism on the cellular density ρ calculated at the steady state in a 0.7% agar simulated gel. The horizontal lines individuate the error band of the experimental values as reported in [2] page 780. Larger values of h_2 corresponds to more efficient apoptotic mass removal.

4 Discussion and conclusions

Validation of the hypotheses introduced in the model has been performed both from a qualitative (Figs. 2, 3) and quantitative (Figs. 4–6) point of view, analyzing both macroscopic (spheroid diameter) and microscopic (densities and activation probabilities) quantities, compared with data on a specific MTS experiment. In modeling the system, we have also reduced the number of computational parameters of the model by estimating some of them and binding others to biological knowledge.

Several of the results presented are in agreement with biological hypotheses proposed in recent experimental papers:

- the fundamental mechanism at the basis of the existence of a steady state is the net balance between proliferation and apoptotic death;
- the qualitative growth dynamics is independent from the host features: the MTS initially grows very slowly, then almost linearly and finally achieves a saturation size;
- the host properties influence the prediction of the spheroid kinetics (see Figs. 7–8), as a result of space occupation and opposition to its subtraction, light lowering in nutrient perfusion and alteration of efficiency in nutrient uptake.

In addition, the results of the in silico growth experiments also allow us to formulate new hypotheses and to make suggestions about new objectives of study:

- the removal of apoptotic corpses play an important role in time and ways of reaching the quiescent configuration (see Fig. 9);
- the general opinion in the scientific community studying tumor growth with MTS is that compactness favors social communication between cells, hence, as reported since about two decades, the survival of more compact MTS to perturbations, like ionizing radiations or cytotoxic drugs, that often act inducing apoptosis. Although our simulations attest that the opposition to growth from the medium has important effects on biochemical processes, it doesn't seem that a real inhibition of apoptosis occurs. In fact, at the steady state $p_d = \frac{1}{2}$, independently from the medium stiffness: $p_d = \frac{1}{2}$ corresponds to $c_s^j(0) = \frac{1}{2}\, c_a^j(0)$ (Eq. (7)), hence $c^{j+1}(0) = c^j(0)$ (Eq. (8)). Nevertheless, the total fraction of apoptotic cells $p_d^j\, p_a^j$ diminishes with the increase of medium stiffness, because the number of activated cells $p_a\, c(0)$ diminishes too (Fig. 6). We suggest that the invariance of p_d at the steady state may be due to the antagonism between deformation and social inhibition of apoptosis, as discussed in Figure 1: much compactness means much closeness between neoplastic cells and higher production of survival signals, but also much deformation, that reduces the efficiency in actual uptake;
- we suggest that the larger resistance of more compact nodules to therapies may be justified by the larger percentage of quiescent cells when the spheroid density is larger, e.g. when the medium rigidity increases.

We thank Prof. P.P. Delsanto (Department of Physics, Politecnico di Torino) and Dr. R. Chignola (Department of Science and Technology, University of Verona) for fruitful discussions and suggestion. M.G. also acknowledges the support from the Compagnia di San Paolo.

References

1. M.T. Santini, G. Rainaldi, P.L. Indovina, Crit. Rev. Onc. Hemat. **36**, 75 (2000)
2. G. Helmlinger, P.A. Netti, H.C. Lichtenbeld, R.J. Melder, R.K. Jain, Nat. Biotechnol. **15**, 778 (1997)
3. G. Eaves, J. Pathol. **109**, 233 (1973)
4. M. Magnano, G. Bongioannini, W. Lerda, B. Capogrosso Sansone, P.P. Delsanto, M. Scalerandi, G.P. Pescarmona, J. Surg. Oncol. **74**, 122 (2000)
5. D. Hanan, J. Folkman, Cell **86**, 353 (1996)
6. M.C. Raff, Nat. **356**, 397 (1992)
7. O. Oudar, Crit. Rev. Onc. Hemat. **36**, 99 (2000)
8. G. Hamilton, Cancer Lett. **131**, 29 (1998)
9. J.A. Adam, N. Bellomo (Eds.), *A survey of models for tumor-immune system dynamics* (Birkhauser, 1997), Chap. 2
10. D. Drasdo, Phys. Rev. Lett. **84**, 4244 (2000)
11. P.P. Delsanto, A. Romano, M. Scalerandi, G.P. Pescarmona, Phys. Rev. E **62**, 2547 (2000)
12. C. Guiot, P.G. Degiorgis, P.P. Delsanto, P. Gabriele, T.S. Deisboeck, J. Theor. Biol. **225**, 147 (2003)
13. M. Scalerandi, B. Capogrosso Sansone, C. Benati, C.A. Condat, Phys. Rev. E **65**, 051918 (2001)
14. L.M. Sander, T.S. Deisboeck, Phys. Rev. E **66**, 051901 (2002)
15. J.D. Humphrey, Proc. R. Soc. London B **459**, 3 (2003)
16. A.F. Jones, H.M. Byrne, J.S. Gibson, J.W. Dold, J. Math. Biol. **40**, 473 (2000)
17. C.Y. Chen, H.M. Byrne, J.R. King, J. Math. Biol. **43**, 191 (2001)
18. B. Capogrosso Sansone, P.P. Delsanto, M. Magnano, M. Scalerandi, Phys. Rev. E **64**, 021903 (2001)
19. D. Ambrosi, F. Mollica, Int. J. Eng. Sci. **40**, 1297 (2002)
20. B. Capogrosso Sansone, M. Scalerandi, C.A. Condat, Phys. Rev. Lett. **87**, 128102 (2001)
21. M. Scalerandi, B. Sansone Capogrosso, Phys. Rev. Lett. **89**, 218101 (2002)
22. M.J. Holmes, B.D. Sleeman, J. Theor. Biol. **202**, 95 (2000)
23. T. Nitta, H. Haga, K. Kawabata, K. Abe, T. Sambogi, Ultramicroscopy **82**, 223 (2000)
24. A.H. Wyllie, Cancer Metast. Rev. **11**, 95 (1992)
25. B. Novak, J.C. Sible, J.J. Tyson, *Checkpoints in the Cell Cycle* (Macmillan Publishers Ltd, 2002), Encyclopedia of Life Sciences. `www.els.net`, pp. 1–8
26. M. Sato, N. Oshima, R.M. Nerem, J. Biomech. **29**, 461 (1996)
27. W. Huicong, W. Ip, R. Boissy, E.S. Grood, J. Biomech. **28**, 1543 (1995)
28. M. Griffa, M. Scalerandi, Phys. Scripta (2004) in press
29. A.H. Wyllie, J.F.R. Kerr, A.R. Currie, Int. Rev. **68**, 251 (1980)
30. M. Scalerandi, A. Romano, G.P. Pescarmona, P.P. Delsanto, C.A. Condat, Phys. Rev. E **59**, 2206 (1999)
31. B. von Tiedemann, U. Bilitewski, Biosens. Bioelectron. **17**, 983 (2002)
32. M. Shibuya, Int. J. Biochem. Cell Biol. **33**, 409 (2001)
33. A. Pluen, P.A. Netti, R.K. Jain, D.A. Berk, Biophys. J. **77**, 542 (1999)
34. R.J. Bold, P.M. Termuhlen, D.J. McConkey, Surg. Oncol. **6**, 133 (1997)
35. R. Chignola, A. Schenetti, G. Andrighetto, E. Chiesa, R. Foroni, S. Sartoris, G. Tridente, D. Liberati, Cell Proliferat. **33**, 219 (2000)
36. B. Alberts, D. Bray, J. Lewis, M. Raff, K. Roberts, J.D. Watson, *Molecular Biology of the Cell,* 3rd edn. (Garland Publishing, 3 edition, 1994)
37. W.H. Goldmann, R. Ezzell, Exp. Cell Res. **226**, 234 (1996)
38. Y.C. Fung, *Biomechanics. Mechanical properties of living tissues*, 2nd edn. (Springer, 1993)
39. V.A. Fadok, Giovanna Chimini, Semin. Imunol. **13**, 365 (2001)
40. L.J. McCawly, L.M. Matrisian, Curr. Biol. **11**, 25 (2001)